ionized species at the interface is balanced by a high partition coefficient and vice versa. All of these conclusions also apply to the case of acidic drugs in an analogous way.

In the study of rat intestinal and gastric absorption of sulfonamides, Koizumi *et al.* (6, 7) derived a first-order rate constant,

$$K_u \sqrt{M} = \frac{abP}{1 + aP} \qquad \text{(Eq. 38)}$$

where M is the molecular weight of the sulfonamide, K_u is the absorption rate of the nonionized moiety, a and b are constants, and P is the partition coefficient.

Equation 38 was found to be in good agreement with a large number of *in situ* experiments. It is noteworthy that the substitution of Eq. 35 or 35*a* into 24 gives

$$K_u = -\frac{AD_R}{Vh} \cdot \frac{BP}{1 + BP} \qquad \text{(Eq. 39)}$$

Both equations have the same form, although the methods of derivation are different. In the next paper, the results of Koizumi *et al.* and others will be discussed and compared with a similar model as presented in this study but modified to simulate the gastric and intestinal membrane.

APPENDIX

Numerical Calculating Procedure—To calculate the change of $(TR)_{-h}$, the concentration profile of R in the lipid phase with time and other parameters, the procedure shown in Scheme I is used. The input data are given in Table I. After $t = 0$, a series of calculation procedures undergo integration for each time increment, $t + \Delta t$. The $(TR)_{-h}$ and (R_i) at time t are determined by the stepwise integration of Eqs. 12–15*a* or 15*b*, depending upon the choice of the perfect-sink or no-sink case, by the Runge-Kutta technique for the initial period, $t \leq 3\Delta t$, and thereafter by the predictor-corrector method of Hamming (10). The calculation of the derivatives in Eqs. 12–15 is performed in the subroutine DRVT after evaluating G in the subroutine CALCG.

The procedure of subroutine CALCG is as follows. The first step involves the calculation of $(H^+)_{-h}$ from the fourth-power polynominal Eq. 16 by the Newton-Raphson method. Then $(R)_{-h}$, $(RH^+)_{-h}$, $(B^-)_{-h}$, and $(HB)_{-h}$ are obtained from Eqs. 1, 2, and 4, respectively. The next step is the evaluation of $(H^+)_{-0}$ from Eq. 17. In turn, $(B^-)_{-0}$, $(HB)_{-0}$, $(RH^+)_{-0}$ and $(R)_{-0}$ are found, using Eqs. 4, 7, and 18 and finally G by Eq. 6.

REFERENCES

(1) A. H. Goldberg, W. I. Higuchi, N. F. H. Ho, and G. Zografi, *J. Pharm. Sci.*, **56,** 1432(1967).

(2) A. Ghanem, W. I. Higuchi, and A. P. Simonelli, *ibid.*, **58,** 165(1969).

(3) S. A. Howard, A. Suzuki, M. A. Farvar, and W. I. Higuchi, to be published.

(4) R. G. Stehle and W. I. Higuchi, *J. Pharm. Sci.*, **56,** 1367(1967).

(5) A. Suzuki, W. I. Higuchi, and N. F. H. Ho, *ibid.*, **59,** 651(1970).

(6) T. Koizumi, T. Arita, and K. Kakemi, *Chem. Pharm. Bull.*, **12,** 413(1964).

(7) *Ibid.*, **12,** 421(1964).

(8) J. Crank, "Mathematics of Diffusion," Oxford, New York, N. Y., 1956.

(9) P. Shore, B. Brodie, and C. Hogben, *J. Pharmacol. Exp. Ther.*, **119,** 361(1957).

(10) A. Ralston and H. Wilf, "Mathematical Methods for Digital Computers," Wiley, New York, N. Y., 1960.

ACKNOWLEDGMENTS AND ADDRESSES

Received July 22, 1969, from the *College of Pharmacy, University of Michigan, Ann Arbor, MI 48104*

Accepted for publication December 16, 1969.

Presented to the Basic Pharmaceutics Section, APhA Academy of Pharmaceutical Sciences, Montreal meeting, May 1969.

Theoretical Model Studies of Drug Absorption and Transport in the Gastrointestinal Tract II

AKIRA SUZUKI*, W. I. HIGUCHI, and N. F. H. HO

Abstract □ Multicompartment diffusional models for the absorption of neutral, acidic, basic, and amphoteric drugs were investigated. The general model consisted of a bulk aqueous phase, an aqueous diffusion layer, n-compartments of homogeneous and heterogeneous phases, and a perfect sink. With the mathematical techniques reported previously, equations were derived in general terms for the nonsteady- and steady-state periods. Utilizing the steady-state diffusion efficiency function of the barrier systems, the first-order rate constants for various examples of two- and three-compartment models were obtained from the general model and some computations were given. Various sets of *in situ* experimental rat data have been analyzed by means of the different models. These include the intestinal, gastric, and rectal absorption of sulfonamides and barbituric acid derivatives. Self-consistent dimensional constants and diffusion coefficients were arrived at and the correlations obtained with the models have been found to be generally satisfactory.

Keyphrases □ Theoretical models—drug absorption, transport, gastrointestinal tract □ Drug absorption, transport, gastrointestinal tract—theoretical models, equations derived □ Kinetics—drug absorption, transport □ Sulfonamides—absorption, diffusion data, rats □ Barbituric acid derivatives—absorption, diffusion data, rats

In a previous paper the diffusion of basic and acidic drugs across an aqueous diffusion layer and a lipid compartment in a homogeneous two-phase model was presented (1). It provided a mathematical technique whereby more complicated models can be handled. A function was also derived which was found useful in analyzing the diffusion rate with respect to the partition coefficient, surface and bulk pH, dissociation constant, diffusion coefficients, and diffusion layer thickness.

In contrast to the two-phase model, this study describes a more general model in an attempt to simulate the diffusion of drug across the biological membrane and is easily adaptable to various conditions as the case may be. It utilizes the same mathematical techniques and computer method of numerical calculation heretofore mentioned. The appropriate theoretical relationships are also applied to some *in situ* experiments on absorption of sulfonamides and barbiturates in the rat intestine, stomach, and rectum.

THEORY

General Description of the Multicompartment Model and Nonsteady-State Diffusion—The general theory involves the simple diffusion in one dimension through multicompartments, each compartment being homogeneous or heterogeneous in phase according to the situation and representing different structural regions of the system (Fig. 1). The first compartment consists of a bulk aqueous phase and a diffusion layer of thickness L_1. The ith compartment ($i = 2, 3 \ldots n$) represents a portion of the membrane having distinct but uniform diffusional characteristics. The present general treatment will be assumed to be heterogeneous, *i.e.*, consisting of aqueous and lipid phases. Its thickness is L_i and the volume fraction of lipid is α_i. After the nth compartment, there is a perfect sink.

Let us now consider the drug also in general terms. The ionic equilibria of an amphoteric drug in water are

$$R_w^+ \overset{K_1}{\rightleftharpoons} R_w^0 + H^+ \overset{K_2}{\rightleftharpoons} R_w^- + 2H^+ \qquad \text{(Eq. 1)}$$

and

$$K_1 = \frac{(R_w^0)(H^+)}{(R_w^+)} \qquad \text{(Eq. 2)}$$

$$K_2 = \frac{(R_w^-)(H^+)}{(R_w^0)} \qquad \text{(Eq. 3)}$$

where (R_w^+), (R_w^-), and (R_w^0) are the concentrations of the cationic, anionic, and unionized drug species, respectively, in water (subscript w); K_1 and K_2 are the dissociation constants; and (H^+) is the hydrogen-ion concentration. For a basic drug, K_1 is its dissociation constant with $K_2 = 0$; for an acidic drug, K_2 is its dissociation constant with $K_1 = \infty$; for a neutral drug, $K_1 = \infty$ and $K_2 = 0$.

In the initial period, one assumes steady-state fluxes in the diffusion layer and nonsteady-state fluxes in the outer compartments. Therefore, applying Fick's first law,

$$G = -D_w^+ \frac{d(R_w^+)}{dx} - D_w^- \frac{d(R_w^-)}{dx} - D_w^0 \frac{d(R_w^0)}{dx} \qquad \text{(Eq. 4)}$$

where G is the total flux of the drug species in the diffusion layer and D is the diffusion coefficient.

The description of the concentration–distance change with time is complex. Each compartment, except the first, is divided into unit cells of equal intervals, Δx_i. The distribution of drug between the lipid and aqueous phases in each cell is assumed to be instantaneously established and follows the Nernst relationship:

$$(R_0^+)_{ij} = P_i^+(R_w^+)_{ij} \qquad \text{(Eq. 5a)}$$

$$(R_0^0)_{ij} = P_i^0(R_w^0)_{ij} \qquad \text{(Eq. 5b)}$$

$$(R_0^-)_{ij} = P_i^-(R_w^-)_{ij} \qquad \text{(Eq. 5c)}$$

where P_i^+, P_i^0, and P_i^- are the partition coefficients of the cationic, nonionic, and anionic species, respectively; and the subscripts i, j, o, and w denote the ith compartment, jth cell, lipid, and aqueous phases, respectively. It is also assumed that the hydrogen-ion concentration in each compartment is constant; *i.e.*, the buffer capacity is large. The total drug concentration Y_{ij} of the jth cell in the ith compartment is

$$Y_{ij} = \alpha_i[(R_0^+)_{ij} + (R_0^0)_{ij} + (R_0^-)_{ij}] + (1 - \alpha_i)[(R_w^+)_{ij} + (R_w^0)_{ij} + (R_w^-)_{ij}] \qquad \text{(Eq. 6)}$$

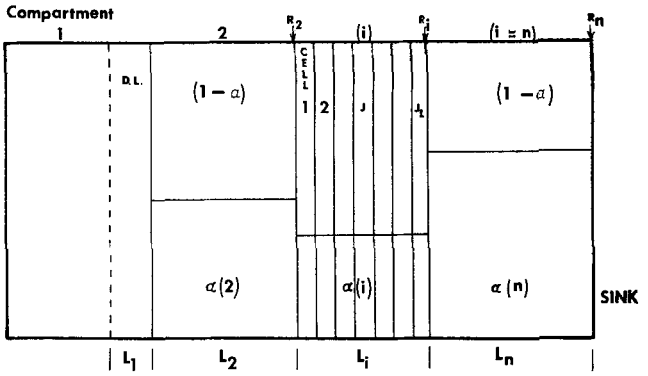

Figure 1—*General diffusion model consisting of an aqueous compartment with a diffusion layer followed by* n *compartments and a perfect sink. Each heterogeneous compartment contains lipid of volume fraction* α *and an aqueous phase* $(1 - \alpha)$. *Each compartment of thickness* L *is subdivided into* j *number of cells.* R *is the ratio of the true interfacial area to the geometrical surface area between compartments.*

From Eqs. 2, 3, 5, and 6, the following are obtained

$$(R_0^+)_{ij} = C_{0,i}^+ \cdot Y_{ij} \qquad \text{(Eq. 7a)}$$

$$(R_0^0)_{ij} = C_{0,i}^0 \cdot Y_{ij} \qquad \text{(Eq. 7b)}$$

$$(R_0^-)_{ij} = C_{0,i}^- \cdot Y_{ij} \qquad \text{(Eq. 7c)}$$

$$(R_w^+)_{ij} = C_{w,i}^+ \cdot Y_{ij} \qquad \text{(Eq. 7d)}$$

$$(R_w^0)_{ij} = C_{w,i}^0 \cdot Y_{ij} \qquad \text{(Eq. 7e)}$$

$$(R_w^-)_{ij} = C_{w,i}^- \cdot Y_{ij} \qquad \text{(Eq. 7f)}$$

where

$$C_{0,i}^+ = P_i^+(H^+)_i^2/\beta_i \qquad \text{(Eq. 8a)}$$

$$C_{0,i}^0 = P_i^0(H^+)_i K_1/\beta_i \qquad \text{(Eq. 8b)}$$

$$C_{0,i}^- = P_i^- K_1 K_2/\beta_i \qquad \text{(Eq. 8c)}$$

$$C_{w,i}^+ = (H^+)_i^2/\beta_i \qquad \text{(Eq. 8d)}$$

$$C_{w,i}^0 = (H^+)_i K_1/\beta_i \qquad \text{(Eq. 8e)}$$

$$C_{w,i}^- = K_1 K_2/\beta_i \qquad \text{(Eq. 8f)}$$

$$\beta_i = \alpha_i[P_i^+(H^+)_i^2 + P_i^0 K_1(H^+)_i + P_i^- K_1 K_2] + (1 - \alpha_i)[(H^+)_i^2 + K_1(H^+)_i + K_1 K_2] \qquad \text{(Eq. 9)}$$

where $C_{w,i}^-$, $C_{w,i}^0$, and $C_{w,i}^+$ are the fractions in the respective anionic, nonionic, and cationic forms of the total concentration of the particular species in the aqueous phase of the ith compartment; and $C_{0,i}^-$, *etc.*, are defined in the same manner. Equations 7–9 indicate that the concentration of drug species in a particular phase of a unit cell, for example, $(R_0^0)_{ij}$, is interdependent with other species in the various phases through Y_{ij} and its magnitude is determined by the coefficient $C_{0,i}^0$, which in turn is directly influenced by the $(H^+)_i$ and the partition coefficient of the species.

The flux from the j to the $j + 1$th cell in the ith compartment is expressed by

$$G_{i(j \to j+1)} = \{\alpha_i[D_0^+(R_{0,ij}^+ - R_{0,ij+1}^+) + D_0^0(R_{0,ij}^0 - R_{0,ij+1}^0) + D_0^-(R_{0,ij}^- - R_{0,ij+1}^-)] + (1 - \alpha_i)[D_w^+(R_{w,ij}^+ - R_{w,ij+1}^+) + D_w^0(R_{w,ij}^0 - R_{w,ij+1}^0) + D_w^-(R_{w,ij}^- - R_{w,ij+1}^-)]\}/\Delta x_i \qquad \text{(Eq. 10)}$$

In terms of the total concentration in the cell, Eq. 10 is rewritten as follows:

$$G_{i(j \to j+1)} = \frac{D_{eff(i)}(Y_{ij} - Y_{i,j+1})}{\Delta x_i} \qquad \text{(Eq. 11)}$$

where the effective diffusion coefficient in the compartment, $D_{eff(i)}$, is

$$D_{eff(i)} = \alpha_i[D_0^+ C_{0i}^+ + D_0^0 C_{0i}^0 + D_0^- C_{0i}^-] + (1 - \alpha_i)[D_w^+ C_{wi}^+ + D_w^0 C_{wi}^0 + D_w^- C_{wi}^-] \qquad \text{(Eq. 12)}$$

Using the finite-difference method and Eq. 11, the nonsteady-state concentration change in the jth cell of the ith compartment with time may be expressed by the following equation,

$$\frac{dY_{ij}}{dt} = \frac{G_{i(j-1\rightarrow j)} - G_{i(j\rightarrow j+1)}}{\Delta x_i} = \frac{D_{\mathrm{eff}(i)}}{(\Delta x_i)^2}(Y_{i,j-1} - 2Y_{ij} + Y_{i,j+1}) \quad (j = 2, 3, 4 \ldots j1 - 1) \qquad \text{(Eq. 13)}$$

Now that the diffusional movement from cell to cell in a compartment has been described, one must further account for the continuity of the flow between compartments by applying the boundary condition that the total flux to the interface is equal to the total flux from the interface. Therefore,

$$G_{T(i\rightarrow i+1)} = \frac{AR_iD_{\mathrm{eff}(i)}}{0.5\Delta x_i}(Y_{i,j1} - Y_{\mathrm{int}(i,i+1)}) = \frac{AR_{i+1}D_{\mathrm{eff}(i+1)}}{0.5\Delta x_{i+1}}(P_{\mathrm{eff}(i,i+1)}Y_{\mathrm{int}(i,i+1)} - Y_{i+1,1}) \qquad \text{(Eq. 14)}$$

where $G_{T(i\rightarrow i+1)}$ is the total flux immediately to or from the boundary, the subscript $j1$ is the last cell of the ith compartment, R_i and R_{i+1} are the ratio of the actual surface area of the ith and $i+1$th compartment, respectively, to the geometrical surface area A and, accordingly, R_i and $R_{i+1} \geq 1$. The $Y_{\mathrm{int}(i,i+1)}$ is the total concentration at the interface on the ith-compartment side and $P_{\mathrm{eff}(i,i+1)}Y_{\mathrm{int}(i,i+1)}$ is the total concentration at the interface on the $i+1$th compartment side where $P_{\mathrm{eff}(i,i+1)}$ is the effective partition coefficient between the respective compartments. Under the assumption that the activity of the unionized drug species on both sides of the boundary is the same, it follows that

$$C_{w,i}{}^0Y_{\mathrm{int}(i,i+1)} = C_{w,i+1}{}^0P_{\mathrm{eff}(i,i+1)}Y_{\mathrm{int}(i,i+1)} \qquad \text{(Eq. 15}a\text{)}$$

and, consequently,

$$P_{\mathrm{eff}(i,i+1)} = \frac{C^0_{w,i}}{C^0_{w,i+1}} \qquad \text{(Eq. 15}b\text{)}$$

The average rate of change in concentration in the last cell of the ith compartment is

$$\frac{dY_{i,j1}}{dt} = \frac{1}{\Delta x_i}\left[G_{i(j1-1\rightarrow j1)} - \frac{G_{T(i\rightarrow i+1)}}{AR_i}\right] \qquad \text{(Eq. 16}a\text{)}$$

and in the first cell of the $i+1$th compartment is

$$\frac{dY_{i+1,1}}{dt} = \frac{1}{\Delta x_{i+1}}\left[\frac{G_{T(i\rightarrow i+1)}}{AR_{i+1}} - G_{i+1,(1\rightarrow 2)}\right] \qquad \text{(Eq. 16}b\text{)}$$

By substitution of Eqs. 11 and 14, the corresponding equations for 16a and b are

$$\frac{dY_{i,j1}}{dt} = \frac{D_{\mathrm{eff}(i)}}{\Delta x_i}\left[\frac{Y_{i,j1-1} - Y_{i,j1}}{\Delta x_i} - \frac{Y_{i,j1} - Y_{\mathrm{int}(i,i+1)}}{0.5\Delta x_i}\right] \qquad \text{(Eq. 17}a\text{)}$$

$$\frac{dY_{i+1,1}}{dt} = \frac{D_{\mathrm{eff}(i+1)}}{\Delta x_{i+1}}\left[\frac{P_{\mathrm{eff}(i,i+1)}Y_{\mathrm{int}(i,i+1)} - Y_{i+1,1}}{0.5\Delta x_{i+1}} - \frac{Y_{i+1,1} - Y_{i+1,2}}{\Delta x_{i+1}}\right] \qquad \text{(Eq. 17}b\text{)}$$

Thus, Eqs. 13, 17a, and 17b describe the nonsteady-state diffusion across the barrier system in a general manner. The method of numerical calculation of the rate and concentration–distance distribution was described previously (1).

Steady-State Diffusion—Previously, the mathematical technique of obtaining the steady-state rate, lag time, and rate constant for the diffusion of drug across a two-phase homogeneous barrier was described under the assumption of an initial quasi-steady-state flux in the aqueous diffusion and a perfect sink. Similarly, one derives the steady-state rate equation,

$$\frac{d(TR)_{w,1}}{dt} = -K_u(TR)_{w,1} \qquad \text{(Eq. 18)}$$

where $(TR)_{w,1}$ is the total concentration of drug in the water phase (Compartment 1) and the rate constant K_u is

$$K_u = \frac{AD_{\mathrm{eff}(1)}}{VL_1} \qquad \text{(Eq. 19)}$$

where V is the volume of the bulk aqueous phase, L_1 is the thickness of the aqueous diffusion layer, and the function f is the diffusion efficiency coefficient of the barriers in the system. In the nonstationary-state period, the function f is time dependent; however, after the lag time, τ, *i.e.*,

$$\tau = 0.5\left[\frac{L_2{}^2}{D_{\mathrm{eff}(2)}} + \frac{L_3{}^2}{D_{\mathrm{eff}(3)}} + 2\frac{(R_2/R_3)L_2L_3}{P_{\mathrm{eff}(2\rightarrow 3)}D_{\mathrm{eff}(3)}}\right] \qquad \text{(Eq. 20)}$$

for a three-compartment model,[1] the f is time independent and is given by the general relationship,

$$f = \frac{L_1/D_{\mathrm{eff}(1)}}{L_1/D_{\mathrm{eff}(1)} + L_2/[R_2P_{\mathrm{eff}(1\rightarrow 2)}D_{\mathrm{eff}(2)}] + L_3/[R_3P_{\mathrm{eff}(1\rightarrow 2)}P_{\mathrm{eff}(2\rightarrow 3)}D_{\mathrm{eff}(3)}] + L_4/[R_4P_{\mathrm{eff}(1\rightarrow 2)}P_{\mathrm{eff}(2\rightarrow 3)}P_{\mathrm{eff}(3\rightarrow 4)}D_{\mathrm{eff}(4)}] + \cdots} \qquad \text{(Eq. 21)}$$

APPLICATION OF THE STEADY-STATE THEORY TO SOME SPECIFIC MODELS

The foregoing general steady-state theory can be applied to some specific multicompartment models. To reiterate some of the assumptions made, (*a*) after a lag period the concentration gradient of the diffusing species in each compartment is linear and, subsequently, (*b*) the drug diffuses across the barriers at a steady-state rate into a perfect sink. The various models are shown in Figs. 2–3 and the lag time can be estimated from Eq. 20 for each model. In addition to the previous assumptions, it is specified that only unionized molecules can partition into the lipid phase, *i.e.*, $P_i{}^+ = P_i{}^- = 0$, and that the aqueous diffusion coefficients in a compartment ($D_{w,i}$) of all ionized and unionized species are equal. Also, let the partition coefficient $P_i{}^0 = P$ and the fraction of undissociated molecules in the aqueous phase in a compartment $X_i = C_{w,i}{}^0$ (see Eq. 8). The effective diffusion coefficient in a compartment ($D_{\mathrm{eff}(i)}$) consisting of a homogeneous phase is simply the diffusion coefficient of the drug in that phase; otherwise, in a heterogeneous compartment it is given by Eq. 12.

With the appropriate substitution of Eqs. 2, 3, 8, 9, 12, 15b, and 21 according to the model into Eq. 19, the absorption rate constant for basic, acidic, or amphoteric drugs can be derived in such a form that is convenient for analysis with experimental data.

Model I: Aqueous–Lipid Compartments—This model consists of a bulk aqueous phase with a diffusion layer and a lipid phase ($\alpha_2 = 1$). With the effective partition coefficient between compartment $P_{\mathrm{eff}(1\rightarrow 2)} = PX_1$ and $D_{\mathrm{eff}(2)} = D_o$, the rate constant is given by

$$K_u = B_1 \cdot \frac{1}{1 + B_2/PX_1} \qquad \text{(Eq. 22)}$$

where

$$B_1 = \frac{AD_{w,1}}{VL_1} \qquad \text{(Eq. 22}a\text{)}$$

$$B_2 = \frac{L_2D_{w,1}}{L_1R_2D_0} \qquad \text{(Eq. 22}b\text{)}$$

Model II: (*a*) Aqueous–Lipid–Aqueous and (*b*) Aqueous–Aqueous–Lipid Compartments—In Model IIa, there are three homogeneous compartments in which the two aqueous phases are separated by a lipid one. The aqueous phases may be of different composition and pH. The relationships, $P_{\mathrm{eff}(1\rightarrow 2)} = PX_1$ and $P_{\mathrm{eff}(2\rightarrow 3)} = 1/PX_3$

[1] For more than three compartments, τ will be of the same form except that the cross terms will be more complicated.

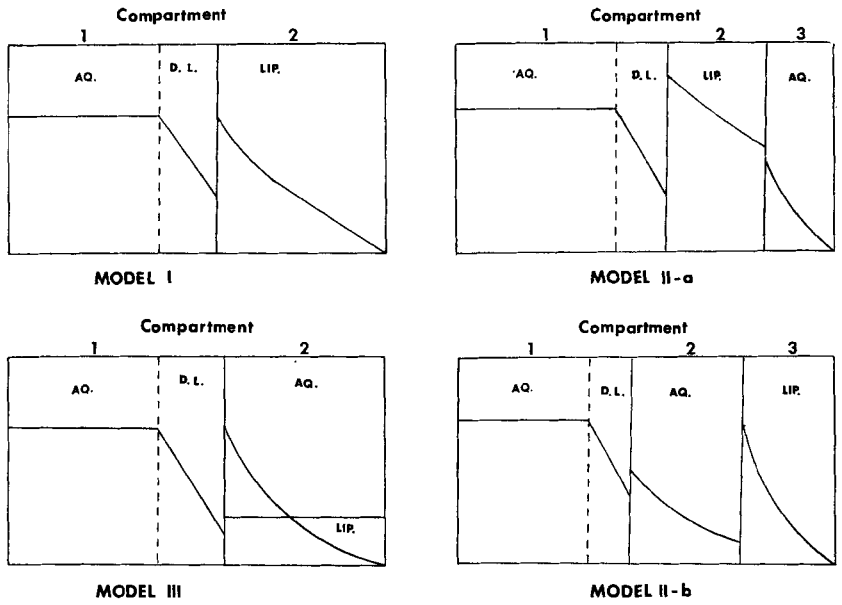

Figure 2—*Some specific models used for the application of the steady-state transport theory.*

are readily derived and, when introduced into Eq. 19,

$$K_u = B_1 \cdot \frac{1}{1 + (B_2/PX_1) + (B_3X_3/X_1)} \qquad \text{(Eq. 23)}$$

where B_1 and B_2 are defined by Eqs. 22*a*, 22*b*, and

$$B_3 = \frac{L_3D_{w,1}}{L_1R_3D_{w,3}} \qquad \text{(Eq. 23}a\text{)}$$

It is noted that the first and second compartments of Model II*a* are the same as in Model I. Comparing Eqs. 22 and 23, the third compartment in the series is accounted for by the addition of a third term in the denominator of the rate-constant equation. The rate-determining factors may be easily deduced by Eq. 23. When the lipid compartment is the rate-determining barrier, the determining factors may be low lipid diffusivity and/or the concentration of unionized drug at the aqueous–lipid interface through X_1 and the partition coefficient. In turn, X_1 depends upon the pH and the nature of the drug, *i.e.*, whether it is amphoteric, acidic, basic, or neutral. Also, if the partition coefficient is high, the transport across the first and the third compartments will be rate determining and the lipid compartment behaves essentially as a control reservoir.

In Model II*b* the sequence of the compartments is different from the previous model. The second aqueous compartment may be thought to be analogous to the presence of a mucoid or thick proteinaceous layer intervening between the bulk aqueous and lipid phases. This model is similar to the membrane described by Robertson (2) in which he assumed that it consisted of phospholipids with a protein envelope. Although identical in form to Eq. 23, the rate-constant equation is

$$K_u = B_1 \cdot \frac{1}{1 + (B_2X_2/X_1) + (B_3/PX_1)} \qquad \text{(Eq. 24)}$$

and the coefficients are

$$B_2 = \frac{L_2D_{w,1}}{L_1R_2D_{w,2}} \qquad \text{(Eq. 24}a\text{)}$$

$$B_3 = \frac{L_3D_{w,1}}{L_1R_3D_0} \qquad \text{(Eq. 24}b\text{)}$$

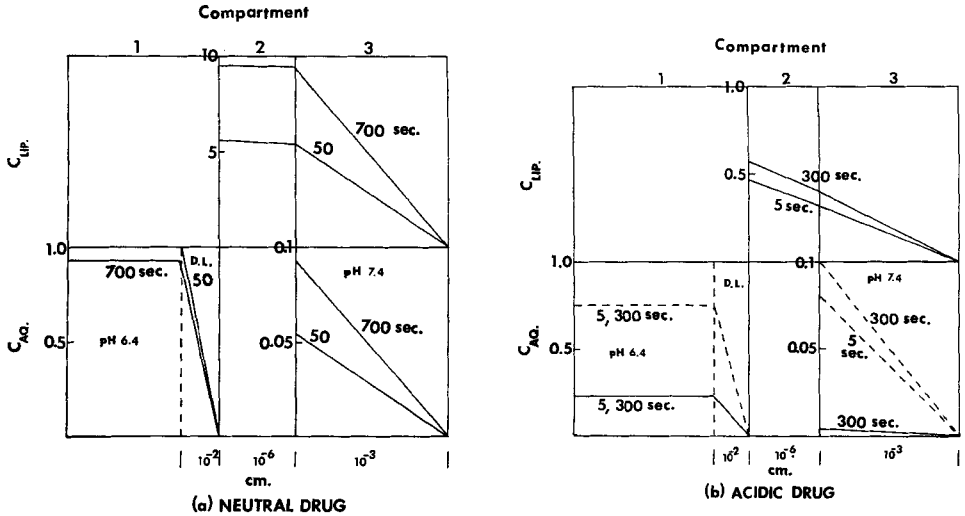

Figure 3—*Time-dependent concentration distribution profiles in the aqueous and lipid phases of Model IV. The model consists of an aqueous compartment followed by lipid and heterogeneous compartments.* V = *10 cm.*^{3}, A = *10 cm.*^{2}, R_2 = *100*, R_3 = *1*, α_1 = *0*, α_2 = *1*, α_3 = *0.1*, D_w = 10^{-6} *cm.*^{2} *sec.*$^{-1}$, D_0 = 10^{-12} *cm.*^{2} *sec.*$^{-1}$, P = *100. In 3a, only a neutral drug is used. In 3b an acidic drug (pKa = 6) is used. Key:* ——, *unionized form; and - - -, ionized form.*

Table I—Comparison Between the Numerically Calculated and Estimated Values of the Lag Time τ and the Steady-State Diffusion Efficiency Coefficient F in Model IV

Drug	$\tau_{calc.}$, sec.	$F_{calc.}$	$\tau_{est.}$,[a] sec.	f
Acidic	10	0.976	8	0.98
Neutral	200	0.90	140	0.90

[a] $\tau_{est.}$ calculated from Eq. 20 and f from Eq. 21.

Table II—Maximum Rate Constant of Gastric Absorption in Rats and Some Physical Constants of Sulfonamides[a]

	Sulfonamide	K_u, hr.$^{-1}$	P[b]	pKa_1	pKa_2
1	Sulfanilamide	0.075	0.36	3.36	10.43
2	Sulfanilacetamide	0.068	0.87	1.78	5.38
3	Sulfaguanidine	0.010	0.03	2.75	12.05
4	Sulfapyridine	0.087	2.24	2.58	8.43
5	Sulfadiazine	0.090	1.54	2.00	6.48
6	Sulfamethoxazole	0.200	22.00	1.76	5.80
7	Sulfathiazole	0.061	0.52	2.36	7.12
8	Sulfamerazine	0.070	2.10	2.26	7.06
9	Sulfisoxazole	0.210	22.40	1.55	5.10
10	Sulfamethizole	0.094	2.20	2.00	5.45
11	Sulfisomidine	0.027	0.40	2.36	7.5
12	Sulfamethazine	0.140	3.61	2.36	7.38
13	Sulfamethoxy-pyridazine	0.079	1.31	2.06	7.00
14	Sulfamono-methoxine	0.200	14.70	2.00	5.90
15	Sulfaethidole	0.180	8.00	1.93	5.60
16	Sulfadimethoxine	0.190	77.80	2.02	6.70
17	Sulfaphenazole	0.200	87.90	1.9	6.50

[a] Data taken from *Reference 4*. [b] P is the partition coefficient of unionized drug between isoamyl alcohol and water at 37°.

Model III: Aqueous-Lipid/Aqueous Compartments—Unlike the previous cases, this model provides for a heterogeneous phase system to simulate a membrane consisting of lipoidal cells in an aqueous intercellular fluid environment. In this way, all molecular species existing in the aqueous diffusion layer are able to permeate through the heterogeneous compartment; however, the rate is determined by the effective permeability coefficient,

$$K_{eff(1\to2)} = P_{eff(1\to2)}D_{eff(2)} = \alpha_2 D_0 P X_1 + (1-\alpha_2)D_{w,2}X_1\left[1 + \frac{(H^+)_2}{K_1} + \frac{K_2}{(H^+)_2}\right] \quad \text{(Eq. 25)}$$

and, with $X_2 = (R_w^0)_2/[(R_w^0)_2 + (R_w^+)_2 + (R_w^-)_2]$ and Eqs. 2–3, it follows that

$$K_{eff(1\to2)} = \alpha_2 D_0 P X_1 + (1-\alpha_2)D_{w,2}\frac{X_1}{X_2} \quad \text{(Eq. 26)}$$

Therefore,

$$K_u = B_1 \cdot \frac{1}{1 + B_2/[PX_1 + B_3(X_1/X_2)]} \quad \text{(Eq. 27)}$$

where B_1 is defined as before,

$$B_2 = \frac{L_2 D_{w,1}}{L_1 R_2 D_0 \alpha_2} \quad \text{(Eq. 27}a\text{)}$$

$$B_3 = \frac{(1-\alpha_2)\,D_{w,2}}{\alpha_2 D_0} \quad \text{(Eq. 27}b\text{)}$$

As the volume fraction of lipid approaches unity ($\alpha_2 \to 1$), the model becomes more like Model I. Higuchi and Higuchi (3) also made a theoretical analysis of the diffusional movement of drugs through heterogeneous barriers; however, their results are somewhat different from the authors'. They also considered the effect of the shape and size of the internal phase and drug interactions with the internal phase.

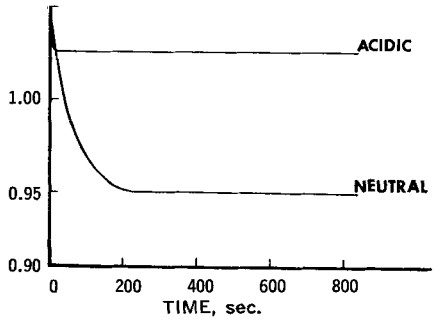

Figure 4—*Change in the function* F *with time during the nonsteady- and steady-state transport of neutral and acidic drugs in Model IV.*

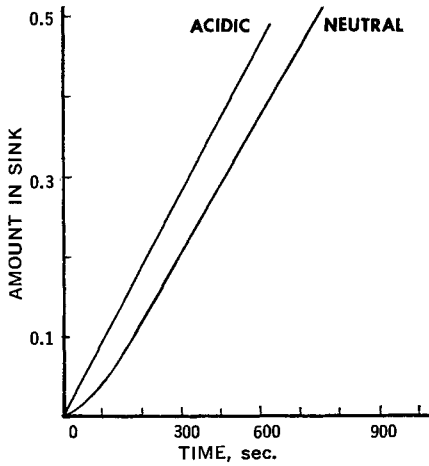

Figure 5—*Total amount of drug accumulated in the perfect sink with time according to Model IV.*

Model IV: Aqueous-Lipid-Lipid/Aqueous Compartments—For this model, consisting of barrier compartments of homogeneous aqueous and lipid phases in series followed by a heterogeneous compartment, or parallel barrier, numerical calculations were performed. Figures 3*a* and *b* show the concentration–distance distribution changes with time for a neutral drug, such as dibutylphthalate or cholesterol, and an acidic drug, pKa = 6. A pH_1 of 6.4 in the bulk aqueous phase and pH_3 of 7.4 in the heterogeneous phase were chosen for their close association with physiological

Table III—Maximum Rate Constants of Gastric Absorption in Rats and Some Physical Constants of Barbituric Acids[a]

	Barbiturate	K_u, hr.$^{-1}$	P[b]	pKa_1
1	Barbital	0.053	3.82	7.91
2	Probarbital	0.082	8.81	8.01
3	Allobarbital	0.092	16.80	7.79
4	Phenobarbital	0.135	34.40	7.41
5	Cyclobarbital	0.142	4.14	7.50
6	Pentobarbital	0.194	106.00	8.11
7	Amobarbital	0.195	113.00	7.94
8	Metharbital	0.178	20.60	8.17
9	Hexobarbital	0.276	73.20	8.34
10	Mephobarbital	0.354	55.80	7.70
11	Thiopental	0.475	991.00	7.45
12	Thiamylal	0.417	1700.00	7.48
13	5-Cyclohexen-1-yl-5-ethyl-1-methylbarbituric acid	0.276	187.00	8.14
14	5,5-Diallyl-1-methylbarbituric acid	0.290	85.50	8.06
15	5-Ethyl-5-iso-pentyl-1-methyl-barbituric acid	0.421	402.00	8.31

[a] Data taken from *Reference 7*. [b] P is the partition coefficient of unionized drug between isoamyl alcohol and water at 37°.

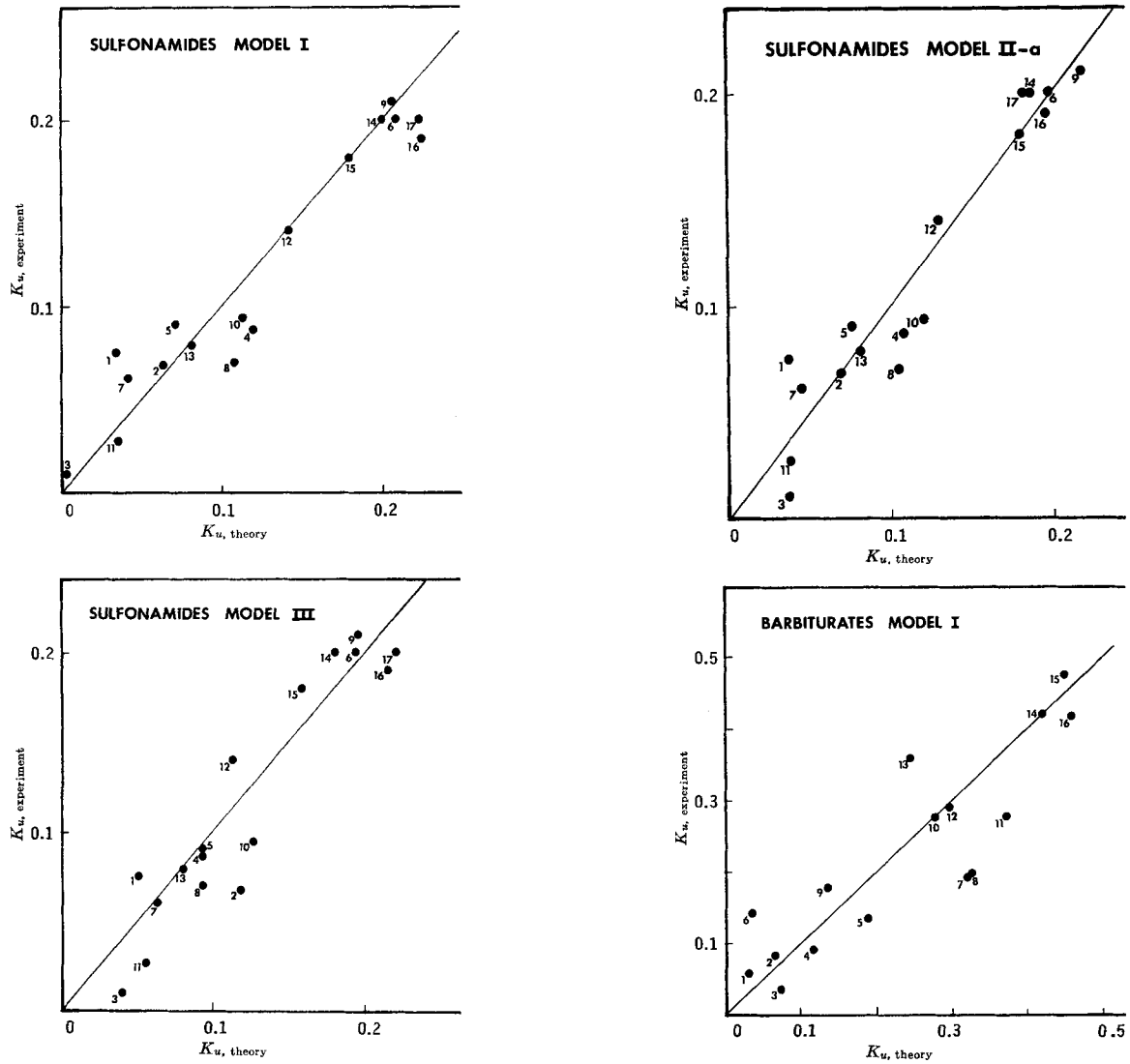

Figure 6—*Comparison of experimental rate constants for the gastric absorption of sulfonamides and barbiturates with the theoretical rate constants calculated for various models using self-consistent dimensional and diffusion constants. Numbers refer to those drugs in Tables II and III.*

conditions. Other dimensional values are given in Fig. 3*a*.

The steady-state rate constant is

$$K_u = B_1 \cdot \frac{1}{1 + (B_2/PX_1) + B_3/[PX_1 + (B_4X_1/X_3)]} \quad \text{(Eq. 28)}$$

where

$$B_3 = \frac{L_3 D_{w,1}}{L_1 R_3 D_{0,3} \alpha_3} \quad \text{(Eq. 28}a\text{)}$$

$$B_4 = \frac{(1 - \alpha_3) D_{w,3}}{\alpha_3 D_{0,3}} \quad \text{(Eq. 28}b\text{)}$$

and B_1 and B_2 are the same as in Eqs. 22*a* and *b*. The magnitude of X_1 and X_3 depends upon the environment of the first and third compartments, respectively, and the nature of the drug.

Between the cases of the acidic and neutral drugs, the total rate of diffusion is slightly faster with the acidic drug. Despite the low concentration of the unionized form of the acidic drug in the bulk aqueous phase, the instantaneous equilibrium conversion of unionized to anionic species at the boundary of the lipid and heterogeneous compartments ($pH_3 - pKa > 1$) and the rapid effective diffusivity of both anionic and nonionic species in the last compartment led to a higher concentration gradient in the lipid than that for the neutral drug case. Thus, the "push-pull" effect is shown. In the case of the neutral drug, the relatively low partitioning from the lipid to the heterogeneous compartment, which is essentially aqueous in character ($\alpha_3 = 0.1$), resulted in a back-up effect or a small lipid concentration gradient.

Figure 4 gives the change in the total rate in the form of $F = (VL_1)/(AD_{w,1}) \cdot K_u$ with time. Previously (1), it was shown that the function F comes from the rigorous numerical calculation of the

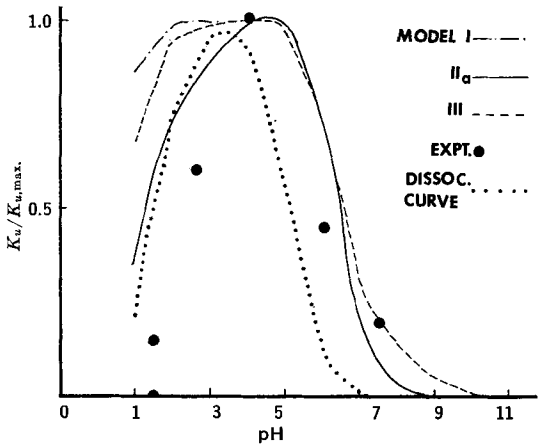

Figure 7—*Comparison of* in situ *and theoretical absorption rates of sulfisoxazole through the intestinal tract from solutions of various pH.*

Table IV—Coefficients of Eq. 22 of Model I Calculated by Regression Analysis of *In Situ* Experimental Absorption Data

Drug	Tract[a]	B_1	B_2
Sulfonamides	*I*	1.87 (1.8)	1.13 (1.0)
Sulfonamides	*G*	0.21 (0.23)	1.91 (2.0)
Barbiturates	*G*	0.43 (0.46)	51.1 (50.0)
Sulfonamides	*R*	1.03 (1.00)	45.1 (41.6)

[a] *I*, *G*, and *R* denote the intestine, stomach, and rectum, respectively. Numerical values of the coefficients in parentheses were calculated using the self-consistent dimensional constants and diffusion coefficients in Table VII.

Table V—Coefficients of Eq. 23 of Model II*a* Calculated by Regression Analysis of *In Situ* Experimental Absorption Data

Drug	Tract	B_1	B_2	B_3
Sulfonamides	*I*	2.25 (2.37)[a]	1.13 (1.0)	0.50 (0.5)
Sulfonamides	*G*	0.247 (0.24)	2.14 (2.0)	0.34 (0.5)
Barbiturates	*G*	0.66 (0.52)	50.0 (50.0)	0.67 (0.5)
Sulfonamides	*R*	1.03 (1.0)	45.1 (42.0)	0.48 (0.5)

[a] Numerical values of the coefficients in parentheses were calculated using the self-consistent dimensional constants and diffusion coefficients in Table VIII.

dynamic flux of drug through the system and the function f is the useful approximation of F in analytic form. At steady state, both F and f should give the same results. The numerical calculations of the lag time τ and the function F at quasisteady state in Table I are in good agreement with the estimated τ (Eq. 20) and f (Eq. 21). Figure 5 shows the total amount of neutral and acidic drug in the sink as a function of time.

APPLICATION OF THEORETICAL MODELS TO ABSORPTION OF SULFONAMIDES AND BARBITURATES IN RATS

In this section an attempt is made to analyze the movement of drugs across cell membranes in the studies of Kakemi *et al.* of the kinetics of absorption of sulfonamides and barbiturates in the intestinal, gastric, and rectal tracts (4–7). Utilizing theoretical models and introducing physical dimensions, some of which are associated with various membranes and others determined by *in vitro* experiments, the authors attempt to calculate for physical constants self-consistent with experimental data and to discuss factors controlling the rate of movement.

Regression Analysis Results and Dimensional Constants—Tables II and III give the experimental results of Kakemi *et al.* only in the gastric absorption of sulfonamides and barbiturates, while the results of intestinal and rectal absorption are found elsewhere

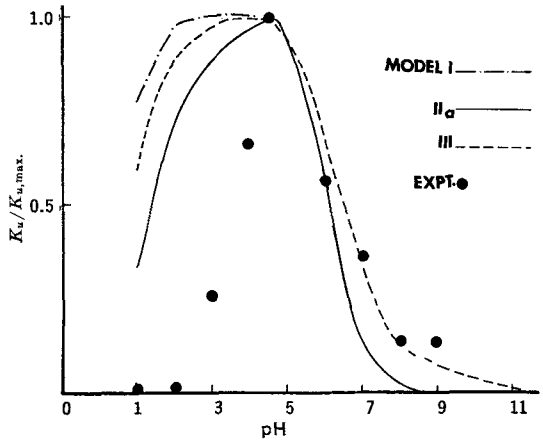

Figure 8—*Comparison of* in situ *and theoretical absorption rates of sulfisoxazole through the stomach from solutions of various pH.*

Table VI—Coefficients of Eq. 27 of Model III Calculated by Regression Analysis of *In Situ* Experimental Absorption Data

Drug	Tract	B_1	B_2	B_3
Sulfonamides	*I*	2.03 (2.0)[a]	3.53 (3.3)	1 03 (1.0)
Sulfonamides	*G*	0.23 (0.25)	4.80 (5.0)	0.95 (1.0)
Barbiturates	*G*	0.46 (0.50)	60.65 (60.7)	1.10 (1.0)
Sulfonamides	*R*	4.23 (4.0)	230.75 (230.0)	1.07 (1.0)

[a] Numerical values of the coefficients in parentheses were calculated using the self-consistent dimensional constants and diffusion coefficients in Table IX.

(5, 6). Their steady-state first-order rate constant,[2] K_u, for an aqueous–lipoidal barrier model has the same general form as Eq. 19, although derived differently. Before applying Models I, II*a*, and III to their results, it is necessary to specify the pH of the compartments following the first bulk aqueous compartment. To account for the possibility of the simultaneous diffusion of buffer species and the subsequent effect on the pH of the aqueous phase in the membrane compartments, it is arbitrarily assumed that $pH_i = (pH_1 + 7.4)/2$, where $i = 2$ or 3 for the respective Model II*a* or III. Also, the volume fraction of lipid in the heterogeneous compartment of Model III was taken to be 0.5. Through the use of (*a*) the values of the maximum experimental K_u, pKa_1, and pKa_2, (*b*) the partition coefficient relative to isoamyl acetate–water, such as those found in Tables II and III, and (*c*)

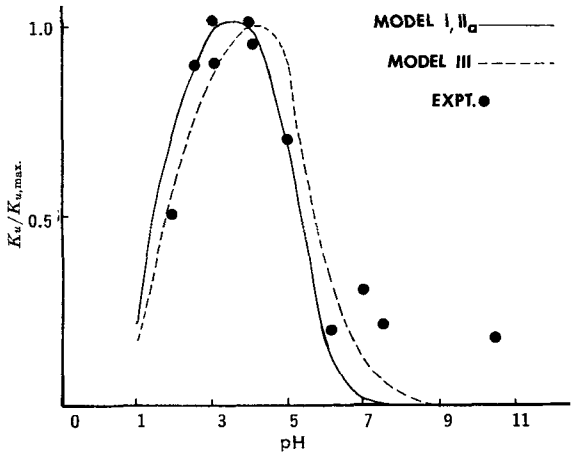

Figure 9—*Comparison of* in situ *and theoretical absorption rates of sulfisoxazole through the rectum from solutions of various pH.*

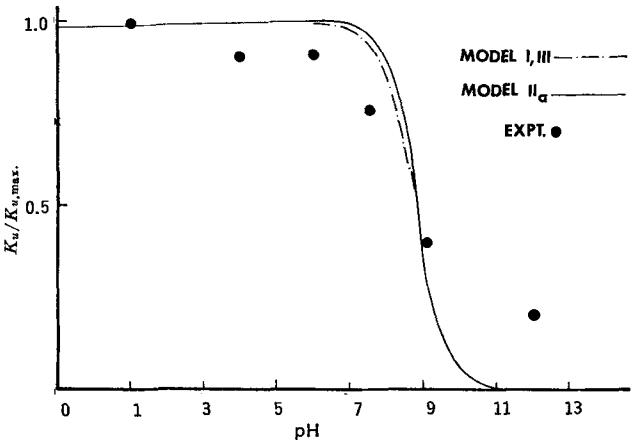

Figure 10—*Comparison of* in situ *and theoretical absorption rates of hexobarbital through the stomach from solutions of various pH.*

[2] According to Kakemi *et al.*, $(M)^{1/2} K_u = (abP)/(1 + aP)$, where a and b are constants, P is the partition coefficient, and M is the molecular weight.

Table VII—Dimensional Constants and Diffusion Coefficients for Model I

Drug	Tract	A/V	L_1	L_2	D_w	D_0	R_2
Sulfonamides	*I*	1	10^{-2}	10^{-6}	5×10^{-6}	10^{-12}	500
Sulfonamides	*G*	0.13	10^{-2}	10^{-6}	5×10^{-6}	10^{-12}	250
Barbituric acid derivatives	*G*	0.13	10^{-2}	10^{-6}	10^{-5}	8×10^{-14}	250
Sulfonamides	*R*	0.56	10^{-2}	10^{-6}	5×10^{-6}	10^{-12}	12

Table VIII—Dimensional Constants and Diffusion Coefficients for Model II*a*

Drug	Tract	A/V	L_1	L_2	L_3	R_2	D_w	D_0
Sulfonamides	*I*	1.3	10^{-2}	10^{-6}	5×10^{-3}	500	5×10^{-6}	10^{-12}
Sulfonamides	*G*	0.15	10^{-2}	10^{-6}	5×10^{-3}	250	5×10^{-6}	10^{-12}
Barbituric acid derivatives	*G*	0.15	10^{-2}	10^{-6}	5×10^{-3}	250	10^{-5}	8×10^{-14}
Sulfonamides	*R*	0.56	10^{-2}	10^{-6}	5×10^{-3}	12	5×10^{-6}	10^{-12}

Table IX—Dimensional Constants and Diffusion Coefficients for Model III

Drug	Tract	A/V	L_1	L_2	R_2	D_0	D_w	$D_{w'}$	α
Sulfonamides	*I*	1.1	10^{-2}	10^{-6}	300	10^{-12}	5×10^{-6}	10^{-12}	0.5
Sulfonamides	*G*	0.14	10^{-2}	10^{-6}	200	10^{-12}	5×10^{-6}	10^{-12}	0.5
Barbituric acid derivatives	*G*	0.14	10^{-2}	10^{-6}	200	1.7×10^{-13}	10^{-5}	1.7×10^{-13}	0.5
Sulfonamides	*R*	2.2	10^{-2}	10^{-6}	4.4	10^{-12}	5×10^{-6}	10^{-12}	0.5

the application of Hartley's method of nonlinear regression analysis (8), the coefficients B_1, B_2, and B_3 of the rate-constant Eqs. 22 (Model I), 23 (Model II*a*), and 27 (Model III) were determined and these are found in Tables IV–VI. From these coefficients, self-consistent combinations of dimensional constants and diffusion coefficients for each model were calculated. To derive the results in Tables VII–IX, the following procedure was taken: (*a*) assume $L_1 = 10^{-2}$ cm., $L_2 = 10^{-6}$ cm., $\alpha = 0.5$ in the case of Model III, and $R_2 = 500$ for the intestinal tract in the case of Model I (9); (*b*) assume $D_{w,1} = 1 \times 10^{-5}$ cm.^{2} sec.$^{-1}$ for the barbituric acid derivatives[3] and by comparing B_1 of the sulfonamides and barbiturates in the gastric tract, take $D_{w,1} = 5 \times 10^{-6}$ cm.^{2} sec.$^{-1}$ for the sulfonamides; (*c*) calculate D_0 for the sulfonamides from B_2 of the intestinal tract, R_2 of the gastric and rectal tract, and the rest of the parameters. Between the barbiturates and the sulfonamides, the $D_{w,1}$ of the latter drug does not seem unreasonable on the basis of the higher average molecular weight. The $D_0 = 1 \times 10^{-12}$ cm.^{2} sec.$^{-1}$ found for the sulfonamides compares well with the diffusion coefficients (10^{-10}–10^{-12} cm.^{2} sec.$^{-1}$) of some organic solutes through lipid bilayer membranes (10) and of various sulfonamides through red blood cells (11). It is observed that the D_0 for the barbiturates is smaller than that for the sulfonamides by a factor of 10. This cannot be easily explained by the usual Stokes-Einstein diffusion equation.

The theoretical K_u of the sulfonamides in the intestinal, gastric, and rectal tracts and of the barbiturates in the gastric tract for the various models was calculated, using the dimensional constants and the diffusion coefficients in Tables VII–IX, and plotted against the K_u of the *in situ* experiments. Figure 6 shows the $K_{u,\text{expt.}}$ *versus* $K_{u,\text{theory}}$ plot only for the gastric absorption of sulfonamides according to Models I, II*a*, and III and of barbiturates for Model I. The strong correlation observed here in these figures was also consistent throughout the other cases. However, at this point one cannot determine which physical model is more applicable, except to say that the constants determined previously are self-consistent.

Comparison of the pH Profile of the Absorption Rate with Experiments and Physical Models—The relative absorption rates *versus* bulk aqueous pH for sulfisoxazole in the intestinal, gastric, and rectal tracts are shown in Figs. 7–9 and for hexobarbital in the gastric tract in Fig. 10. The calculated results of the physical models are compared with experimental data.

In the cases of gastric and intestinal absorption of sulfisoxazole, the physical models show a large deviation in the acidic region and a relatively good fit on the alkaline side of the profile, particularly with Model III. The profile of Model I is symmetrical about the dissociation curve. This is not surprising in view of the lengthy discussion given earlier (1). On the other hand, asymmetry of the profiles of Models II*a* and III about the dissociation curve is found. This is explainable by the influence of the effective pH in the aqueouslike compartments of the membrane, which was assumed to be the arithmetic average of the pH of the bulk drug solution and the physiologic pH of 7.4 on the distribution and transport of drug species in the membrane.

Because of the restriction that the (H^+) in any compartment (particularly, the first compartment) is constant, the present models cannot adequately account for the shift of the maximum experimental rates in Figs. 7 and 8 to higher pH values of the bulk solution relative to the pH of the dissociation curve at which the fraction of the unionized drug form is maximum. There is experimental evidence[4] in the case of gastric absorption of sulfisoxazole that increasing the buffer capacity of the drug solution tends to shift the maximum rate closer to the pH maximum of the dissociation curve. Thus, an accurate accounting of the pH at the surface and within the aqueous phases of the membrane and also protein binding in the physical models may explain the shift of the experimental maximum rate to the more alkaline side. Although there can be a difference between the surface and bulk solution pH, it seems doubtful that they are related through the surface potential (12) in *in situ* experiments; that is, $pH_s = pH_{soln.} + e\psi_0/kT$. Instead it is suggested that surface pH might be related to acid production in the cells and diffusion into the bulk solution.[5]

In the absorption rate *versus* bulk pH profile for the rectal absorption of sulfisoxazole (Fig. 9) and gastric absorption of hexobarbital (Fig. 10), there was relatively good agreement between the *in situ* experimental results and physical models. Maximum absorption of sulfisoxazole was observed at the isoionic point and the absorption rate of hexobarbital corresponded with the pKa.

In conclusion it is difficult to select the physical model that best describes the *in situ* absorption experiments in the intestinal, gastric,

[3] Kakemi *et al.* found $D_{w,1} = 0.815 - 1.27 \times 10^{-5}$ cm.^{2} sec.$^{-1}$ at 37° for the barbiturates.

[4] Refer to Fig. 5 in *Reference 4*.

[5] Theoretical models involving the effect of the surface potential on the one hand and acid production with simultaneous reaction and diffusion on the other hand are being investigated.

or rectal tracts since all of the models studied showed fairly good agreement. More knowledge of the structure and microenvironment of the membrane as well as drug interactions with cellular substances is necessary before modification of the physical models can be made. Furthermore, the models generally have more quantitative parameters in detail which the usual *in situ* experiments alone cannot provide. However, the physical model approach to drug transport studies is being further investigated.

REFERENCES

(1) A. Suzuki, W. I. Higuchi, and N. F. H. Ho, *J. Pharm. Sci.*, **59,** 644(1970).

(2) J. Kavanau, "Structure and Function of Biological Membranes," vol. I, Holden-Day, San Francisco, Calif., 1965, p. 145.

(3) W. I. Higuchi and T. Higuchi, *J. Amer. Pharm. Ass., Sci. Ed.*, **49,** 568(1960).

(4) T. Koizumi, T. Arita, and K. Kakemi, *Chem. Pharm. Bull.*, **12,** 413(1964).

(5) *Ibid.*, **12,** 421(1964).

(6) K. Kakemi, T. Arita, and S. Muranishi, *ibid.*, **13,** 861(1965).

(7) K. Kakemi, T. Arita, R. Hori, and R. Konishi, *ibid.*, **15,** 1534(1967).

(8) N. R. Draper and H. Smith, "Applied Regression Analysis," Wiley, New York, N. Y., 1966, p. 269.

(9) T. H. Wilson, "Intestinal Absorption," W. B. Saunders, Philadelphia, Pa., 1962.

(10) R. C. Bean, W. C. Shepperd, and H. Chan, *J. Gen. Physiol.*, **52,** 495(1968).

(11) L. B. Holder and S. L. Hayes, *Mol. Pharmacol.*, **1,** 266 (1965).

(12) A. Albert, *Pharmacol. Rev.*, **4,** 136(1952).

ACKNOWLEDGMENTS AND ADDRESSES

Received September 23, 1969, from the *College of Pharmacy, University of Michigan, Ann Arbor, MI 48104*

Accepted for publication October 30, 1969.

Presented to the Basic Pharmaceutics Section, APhA Academy of Pharmaceutical Sciences, Montreal meeting, May 1969

* Present address: Tanabe Seiyaku, Osaka, Japan.

Interfacial Barriers in Interphase Transport III: Transport of Cholesterol and Other Organic Solutes into Hexadecane–Gelatin–Water Matrices

ABDEL-HALIM GHANEM, W. I. HIGUCHI, and A. P. SIMONELLI

Abstract □ The purpose of this study was to quantitate the transport behavior of several organic solutes in matrix systems composed of micron-size hexadecane droplets dispersed in an aqueous gelatin gel where the oil–water interfacial barrier to transport was expected to play an important role. Two interrelated experiments were conducted. The first was the one-dimensional aqueous uptake of the solute by the matrix which was a continuous layer placed at the bottom of a beaker. The other experiment was solute uptake and release from aggregates of oil droplets suspended in an aqueous medium. Solutes investigated were ^{14}C-labeled cholesterol, diethylphthalate, ^{14}C-labeled octanol, and ^{14}C-labeled progesterone. The data have been analyzed by various physical models. It was found that cholesterol transport essentially was controlled by the oil–water interfacial barrier in both kinds of experiments—even when the matrix thickness was as large as 3.7 mm. For the other solutes, the oil–water interfacial barriers were found to be controlling in the experiments with aggregates (10–1000 μ). However, in the experiments with the continuous matrix layers, bulk matrix diffusion factors as well as the oil–water interphase transport were found to be important for these solutes. The techniques developed in this investigation should be useful: (*a*) in the quantitation of interfacial barriers in oil–water interphase transport of solutes, and (*b*) in the separation of various bulk diffusional resistances from interfacial resistances in complex multiphase matrices.

Keyphrases □ Interphase transport—interfacial barriers □ Hexadecane–gelatin–water matrix—organic solute transport □ Matrix layer—solute uptake □ Aggregated gelatin encapsulated hexadecane droplets—solute transport □ Electrolyte, polysorbate 80, concentration effects—interphase transport

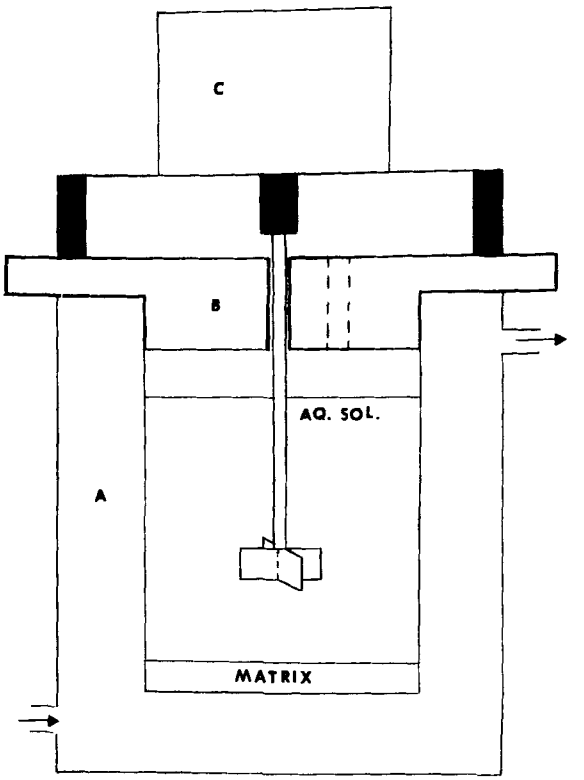

Figure 1—*Schematic diagram showing the apparatus used for the continuous matrix layer (CML) uptake experiments.*

Recent studies in these laboratories have been aimed at the mechanistic understanding of various factors influencing the interphase transport of drugs and other biologically interesting substances. These investigations (1–4) have considered, for example, the simultaneous multiphase interactions involving pH and the buffer parameters, the oil–water partition coefficients, and the diffusion coefficients. More recently (5–8), utilizing a novel technique, the existence and the importance of the